THE JOURNAL OF BIOLOGICAL CHEMISTRY VOL. 289, NO. 47, pp. 32694–32702, November 21, 2014

Connexin 46 (Cx46) Gap Junctions Provide a Pathway for the Delivery of Glutathione to the Lens Nucleus*[S]

Received for publication, July 17, 2014, and in revised form, October 2, 2014 Published, JBC Papers in Press, October 7, 2014, DOI 10.1074/jbc.M114.597898

Nefeli Slavi[‡], Clio Rubinos[‡], Leping Li[§], Caterina Sellitto[§], Thomas W. White[§], Richard Mathias[§], and Miduturu Srinivas[‡1]

From the [‡]Department of Biological and Vision Sciences and the Graduate Center for Vision Research, State University of New York College of Optometry, New York, New York 10036 and the [§]Department of Physiology and Biophysics, State University of New York, Stony Brook, New York 11794

Background: Delivery of the anti-oxidant, glutathione, to the lens nucleus is vital for its transparency.
Results: Gap junction channels, which couple central fiber cells to outer lens cells, are permeable to glutathione.
Conclusion: Glutathione diffuses from cortical cells to the nucleus via gap junctions.
Significance: The age-dependent decline of glutathione levels, an initiating factor in cataract formation, might be due to alterations in coupling.

Maintenance of adequate levels of glutathione (GSH) in the lens nucleus is critical for protection of lens proteins from the effects of oxidative stress and for lens transparency. How GSH is transported to the nucleus is unknown. We show that GSH diffuses to the nucleus from the outer cortex, where a high concentration of the anti-oxidant is established by synthesis or uptake, via the network of gap junctions. Using electrophysiological measurements, we found that channels formed by Cx46 and Cx50, the two connexin isoforms expressed in the lens, were moderately cation-selective (P_{Na}/P_{Cl} ~5 for Cx46 and ~3 for Cx50). Single channel permeation of the larger GSH anion was low but detectable (P_{Na}/P_{GSH} ~12 for Cx46 and ~8 for Cx50), whereas permeation of divalent anion glutathione disulfide (GSSG) was undetectable. Measurement of GSH levels in the lenses from connexin knock-out (KO) mice indicated Cx46, and not Cx50, is necessary for transport of GSH to the core. Levels of GSH in the nucleus were markedly reduced in Cx46 KO, whereas they were unaffected by Cx50 KO. We also show that GSH delivery to the nucleus is not dependent on the lens microcirculation, which is believed to be responsible for extracellular transport of other nutrients to membrane transporters in the core. These results indicate that glutathione diffuses from cortical fiber cells to the nucleus via gap junction channels formed by Cx46. We present a model of GSH diffusion from outer cells to inner fiber cells through gap junctions.

Age-related nuclear cataract is a leading cause of blindness in the world. A key initiating factor in the formation of age-related cataracts is the abrupt reduction in the levels of glutathione in the lens nucleus. GSH, a monovalent anionic tripeptide, is the principal antioxidant in the lens and maintains protein thiols in a reduced state (1, 2). Levels of GSH are high in the epithelium and in outer differentiating fibers where the anti-oxidant is synthesized from the amino acids cysteine, glutamate, and glycine by the enzymes γ-glutamylcysteine synthetase and glutathione synthetase (3, 4). A high ratio of GSH to GSSG here is maintained by the enzymatic action of glutathione reductase, whose activity is greatest in the outer cortex (3, 4). In contrast, levels of GSH are lower in the lens nucleus (1, 5–7), due to utilization and the much reduced activity of enzymes involved in its synthesis and regeneration. The regional variation in GSH levels is known to worsen with age, making proteins in the lens nucleus highly susceptible to the effects of reactive oxygen species, leading to formation of protein-mixed disulfides and high molecular weight aggregates and nuclear cataracts (8–11).

The mechanism by which GSH is transported to the lens nucleus is not clear. The lens maintains an internal circulating current that generates a circulation of fluid (12). which brings metabolites like glucose into the lens core from the aqueous humor. The circulating current is primarily carried by sodium ions and enters the lens along the extracellular spaces between cells (13, 14). After crossing the fiber cell membranes in the lens interior, it flows from cell to cell toward the surface through a gap junction-mediated pathway (13, 14). The high concentration of gap junction channels at the equator causes the intracellular current to be directed to surface cells (15), where Na^+/K^+ pumps located in epithelial cells transport the sodium out of the lens. The circulating ionic current generates fluid flow through gap junctions. Passive gap junction-mediated intracellular fluid flow is driven by hydrostatic pressure, which is highest in lens central cells and lowest in the peripheral cells (16). Solutes such as glucose are carried by extracellular water flow and are taken up into inner fiber cells by membrane glucose transporters (17). Anti-oxidants such as GSH might be carried to the lens core in a similar fashion, although uptake transporters for GSH in the nucleus have not yet been identified.

An alternative view is that GSH diffuses from the outer cortex to the nucleus via gap junction channels. This view was based on a study that followed the movement of ^{35}S-labeled cysteine in the lens (18, 19). Movement of the label, which was

* This work was supported, in whole or in part, by National Institutes of Health Grants EY006391 (to R. T. M.), EY013163 (to T. W. W.), and EY13869 (to M. S.).
[S] This article contains supplemental Fig. 1.
[1] To whom correspondence should be addressed: Dept. of Biological and Vision Sciences and the Graduate Center for Vision Research, State University of New York College of Optometry, 33 W. 42nd St., New York, NY 10036. Tel.: 212-938-5571; Fax: 212-938-5794; E-mail: msrinivas@sunyopt.edu.

incorporated into GSH, occurred in the equatorial plane along the length of fiber cells where gap junctions are abundantly expressed. A barrier to diffusion of GSH was shown to develop with age, leading to a decrease in GSH delivery to the lens core (19). Diffusion of anionic GSH through gap junctions is driven by the large concentration gradient from the surface to the center as well as by the relatively depolarized resting membrane potential of inner fiber cells (V_m ~−50 mV) compared with outer fiber cells (V_m ~−70 mV) (14). Gap junctional coupling in fiber cells is provided by two connexin isoforms, Cx46 and Cx50 (20–23). In the outer cortex, coupling is provided by both Cx46 and Cx50, with each connexin contributing roughly 50% of the total conductance (~1 siemens/cm^2), whereas in mature fiber cells the coupling conductance is dominated by Cx46 gap junctions (20, 24–26).

The purpose of this study was to determine the pathway by which GSH is transported to the lens core. Diffusion of the anti-oxidant from the cortex to the nucleus is mainly dependent on the permeability of gap junctions formed by Cx46 and, to a lesser extent Cx50, to GSH. The extent to which the two lens gap junction channels allow the passage of GSH is not known. Therefore, we first examined the permeation of anions (Cl^- and GSH^-) through channels formed by Cx46 and Cx50 using electrophysiological measurements in exogenous expression systems. Next, we determined the influence of gap junctional permeability of GSH on the levels of the anti-oxidant in the lens core. Specifically, we measured the levels of the anti-oxidant in Cx46 and Cx50 KO mice. Finally, we examined the contribution of the lens microcirculation to the delivery of GSH. Our results indicate that Cx46-mediated intercellular diffusion of GSH from the outer cortex is a major source by which the lens nucleus receives its supply of the important anti-oxidant.

EXPERIMENTAL PROCEDURES

Transient Transfection of Mammalian Cells—Mouse neuroblastoma (N2A) cells were cultured in Dulbecco's modified Eagle's medium (DMEM) (Invitrogen) supplemented with 10% fetal bovine serum and 1% penicillin/streptomycin. Cells were transiently transfected with 400 ng of Cx43, Cx46, or Cx50 cDNAs in combination with mCherry plasmid (Clontech) with Lipofectamine 2000 reagent (Invitrogen), according to the manufacturer's instructions. DNA concentrations were measured using Nanodrop 2000 (Thermo Scientific). Cells were plated at low density onto glass coverslips.

Expression of Cx46 and Cx50 Hemichannels in Xenopus Oocytes—RNA was synthesized and oocytes were prepared and injected as described previously (27). Injected oocytes were maintained at 16–18 °C in a modified ND96 solution containing (in mM) 100 NaCl, 2 KCl, 1 $MgCl_2$, 1.8 $CaCl_2$, 10 glucose, 10 HEPES, 5 pyruvate, pH adjusted to 7.6. For patch clamp recordings of Cx46 and Cx50 hemichannel currents, *Xenopus* oocytes were manually devitellinized in a hypertonic solution consisting of (in mM) 220 sodium aspartate, 10 KCl, 2 $MgCl_2$, and 10 HEPES and then placed in the ND96 solution with no added $CaCl_2$.

Experimental Animals—Genetically modified mice used in this study included Cx46 knock-out (Cx46 KO) and Cx50 knock-out (Cx50 KO) (23, 28). All mice were in a C57BL genetic background. In this background, genetic ablation of Cx46 leads to formation of far milder cataracts (29). For all experiments, 1–6-month-old animals were used, as specified in the text. Animals were euthanized by CO_2 inhalation; their eyes were enucleated, and the lenses were dissected.

Measurement of GSH Levels—Whole lenses were dissected, weighed, and homogenized in ice-cold phosphate-buffered saline (PBS). In majority of experiments, lenses were separated into two fractions, with one fraction containing the epithelium and outer cortex and other containing the nucleus, and homogenized in 300 and 100 μl of PBS, respectively. Samples were centrifuged at 4 °C for 15 min at 10,000 rpm. For deproteination, equal volumes of 10% metaphosphoric acid were added to the supernatants, and samples were centrifuged at 4 °C for 10 min at 10,000 rpm. GSH was measured in deproteinated supernatants using the glutathione assay kit (Cayman Chemical Co., Ann Arbor, MI) according to manufacturer's instructions. For experiments in which the lens circulation was inhibited, whole lenses were incubated for 3 h at 37 °C in artificial aqueous humor (AAH)[2] or AAH supplemented with Na^+/K^+ pump inhibitor ouabain (1 mM) or Na^+-free AAH before the GSH assay. AAH contained (in mM) 130 NaCl, 5 KCl, 5 $NaHCO_3$, 1 $CaCl_2$, 0.5 $MgCl_2$, 5 glucose, 20 HEPES.

Electrophysiological Recordings and Data Analysis—All electrophysiological measurements were obtained using Axopatch 1D patch clamp amplifiers (Axon Instruments, Foster City, CA). Data were acquired by using pCLAMP9.2 software (Molecular Devices, CA); analysis was performed with pCLAMP9.2 and ORIGIN 6.0 software (Microcal Software, Northampton, MA). Single channel currents were filtered at 0.5–1 kHz and sampled at 2–5 kHz.

Junctional currents were measured between N2A cell pairs using the dual whole cell voltage clamp technique as described previously (30). Single channel currents were investigated in weakly coupled cell pairs (1 or 2 channels) without the use of uncoupling agents by applying voltage ramps to one cell of a pair. The solution bathing the cells contained (in mM) 140 NaCl, 5 KCl, 2 CsCl, 2 $CaCl_2$, 1 $MgCl_2$, 5 HEPES, 5 dextrose, 2 pyruvate, and 1 $BaCl_2$, pH 7.4. Patch electrodes had resistances of 3–5 megohms when filled with internal solution containing (in mM) 140 NaCl, 5 EGTA, 1 $CaCl_2$, and 10 HEPES, pH 7.2. In experiments involving ionic substitutions, NaCl was replaced by equimolar amounts of sodium salts of different anions. Pipette solutions containing NaGSH were prepared in deoxygenated distilled water (bubbled with 100% nitrogen for one h) on ice and immediately stored at −80 °C in 1-ml aliquots. Solutions were aspirated into a gas-tight Hamilton syringe before use.

For reversal potential measurements of gap junction channel currents, one patch pipette solution consisted of (in mM) 150 NaGSH (or NaCl), 5 EGTA, and 5 HEPES, pH 7.3. The other patch pipette was filled with the same solution except that NaGSH (or NaCl) was reduced to 50 mM with PEG-600 added to balance osmolarity. The Ag-AgCl wire was connected to the

[2] The abbreviation used is: AAH, artificial aqueous humor.

bath via a 3 M KCl agar bridge. The pipette Ag-AgCl wire was connected to a 3 M KCl-containing agar bridge (3% agarose) inside the pipette holder. Amplifier offsets were nulled with the tips of the pipettes in a stream of 1 M KCl solution to minimize the liquid junction potentials between the different pipette solutions and the bath solution. After correcting the offset, whole cell recordings of cell pairs were obtained to measure junctional currents. Voltage ramps from −100 to +100 mV were applied to one cell of a pair, and the junctional current was recorded from the second cell. Reversal potentials were measured by applying voltage ramps to one cell of a pair. All measurements were done in weakly coupled cell pairs (<1 nS) to ensure that gradients do not collapse due to mixing of pipette solutions between coupled cells. The baseline membrane currents for each cell were measured by manually separating cells at the end of the recording and were subtracted from the junctional current. Activity coefficients were used in the Goldman-Hodgkin-Katz equation for calculation of permeability ratios of anions relative to Na^+ (P_{Na}/P_{anion}) from the changes in the reversal potential, E_{rev}. The permeability ratios for GSH were calculated by assuming that it has the same activity coefficient as Cl^-.

Reversal potentials of single Cx46 and Cx50 hemichannel currents in *Xenopus* oocytes were obtained by exposing excised inside-out patches to 4:1 salt gradients. The pipette solution contained 100 NaGSH (or 100 NaCl), 5 EGTA, 1 $MgCl_2$, 1 $CaCl_2$, and 5 HEPES, pH 8.0. The bath contained the same solution, except that NaGSH (or NaCl) was increased to 400 mM in some experiments. All other experimental procedures, including correction of liquid junction potentials and calculation of permeability ratios, were performed as described above.

RESULTS

GSH Permeability of Cx46 and Cx50 Channels—For a large aqueous pore such as those formed by connexin channels, unitary conductance is dependent on the aqueous mobility of the ion, assuming that the movement of ions in the channel is independent (31). To obtain a qualitative estimate of anionic flux through gap junctions formed by Cx46 and Cx50, we measured single channel conductances with patch pipettes containing 140 mM sodium salts of chloride, glutamate, ascorbate, and GSH anions. The aqueous mobilities of these anions follows the sequence chloride > glutamate > ascorbate > GSH. The effect of replacement of Cl^- with larger anions on the single channel conductance of gap junctions formed by Cx43 was also measured in comparison, as it is known to form nonselective channels (31, 32). Single channel current voltage relations for Cx43, Cx46, and Cx50 gap junctions in different sodium salts were generated by application of voltage ramps between −100 to +100 mV to one cell of a pair. Fig. 1*A* shows a representative recording from a Cx50-expressing cell pair in NaCl and NaGSH. Replacement of Cl^- with GSH did not affect channel gating or the open and closed time distributions (data not shown). Equimolar replacement of Cl^- with progressively larger anions caused a decrease in unitary conductance of Cx43, Cx46, and Cx50 gap junction channels (Table 1). However, as shown in Fig. 1*B*, the magnitudes of decrease in single channel conductance were dependent on the connexin subtype.

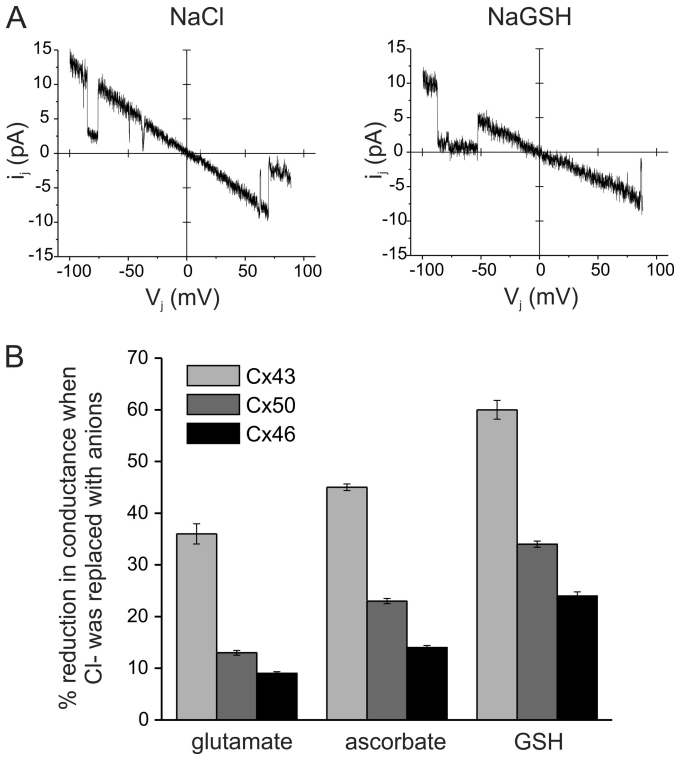

FIGURE 1. **Effect of large anions on single channel conductance of Cx43, Cx46, and Cx50 gap junctions.** *A,* single channel current-voltage relations from Cx50-expressing cells in symmetric 140 mM NaCl or NaGSH internal solutions. Currents were recorded in response to voltage ramps from +100 to −100 mV. Replacement of chloride with GSH in the recording solution reduced the Cx50 single channel conductance without affecting gating. Single channel conductances of Cx43, Cx46, and Cx50 gap junctions in different sodium salts were measured from *I-V* relations and collectively presented in Table 1. *B,* reduction in conductance when Cl^- was replaced with larger anions. The single channel conductance of Cx43, Cx46, and Cx50 junctional channels was reduced in a manner proportional to their aqueous diffusion coefficients. The magnitudes of the decrease were largest for Cx43 but lower for Cx46 and Cx50, suggesting differences in charge selectivity. Reductions were calculated from the results presented in Table 1.

TABLE 1

Single channel conductances of Cx43, Cx46, and Cx50 measured with patch pipettes containing 140 mM of sodium salts

Values are means ± S.E. from 5 to 10 cell pairs for each condition.

Sodium salt	Cx43	Cx46	Cx50
Cl^-	89.7 ± 1.6	94.9 ± 2.3	144.1 ± 1.9
$Glutamate^-$	57.1 ± 3.1	86.5 ± 3.3	125.2 ± 4.4
$Ascorbate^-$	49.3 ± 0.7	81.7 ± 2.3	111.1 ± 2.4
GSH^-	36.2 ± 1.1	67.5 ± 1.9	95.7 ± 1.7

Replacement of Cl^- with glutamate and GSH reduced conductance of Cx43 gap junction channels by ~ 40 and 60%, respectively (Fig. 1*B*). In contrast, the single channel conductance of Cx46 and Cx50 channels changed by only 7 and 15%, respectively, when patch pipettes contained sodium glutamate instead of NaCl. Similarly, replacement of Cl^- with GSH reduced the unitary conductance of Cx46 and Cx50 channels by only 14 and 32%, respectively (Table 1). These results suggest that the conductance in Cx46 is dominated by cations, whereas in Cx43 it is provided by both anions and cations. Cx50 channels also appear to display a higher selectivity for cations although to a lower extent compared with Cx46.

We measured reversal potentials in single salt gradients to obtain a more precise estimate of anionic permeability of chan-

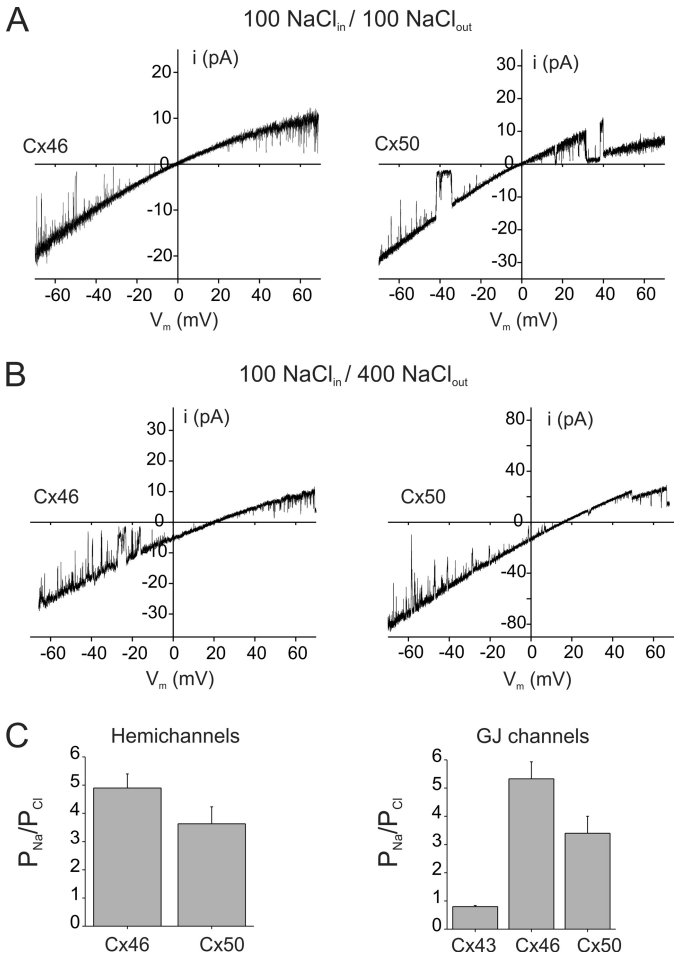

FIGURE 2. **Cx46 and Cx50 form cation-preferring channels.** *A* and *B,* single channel current-voltage relations for Cx46 (*left*) and Cx50 (*right*) hemichannels in symmetric NaCl solutions (*A*) or 100:400 asymmetric NaCl solutions (*B*). Cx46 and Cx50 hemichannel currents were recorded from excised inside-out patches in response to 8-s voltage ramps applied between −70 and +70 mV. In symmetric NaCl solutions, Cx46 and Cx50 currents show inward rectification and reversed polarity at 0 mV. In asymmetric NaCl solutions, reversal potentials for Cx46 and Cx50 hemichannel currents are shifted toward the equilibrium potential for Na^+, indicating a lower permeability to Cl^- relative to Na^+. Inward rectification of the currents also increased in asymmetric solutions, consistent with the presence of higher Na^+ concentration on the extracellular side. *C,* permeability ratios (P_{Na}/P_{Cl}) of hemichannels (*left*) and gap junction channels (*right*) formed by connexins expressed in the lens. P_{Na}/P_{Cl} values for hemichannels and gap junction channels were calculated from reversal potentials in asymmetric 4:1 and 3:1 NaCl gradients, respectively. Hemichannels and gap junction channels formed by Cx46 and Cx50 are moderately selective for Na^+ over Cl^-. In comparison, Cx43 forms nonselective channels. Values represent the means ± S.E. from multiple recordings.

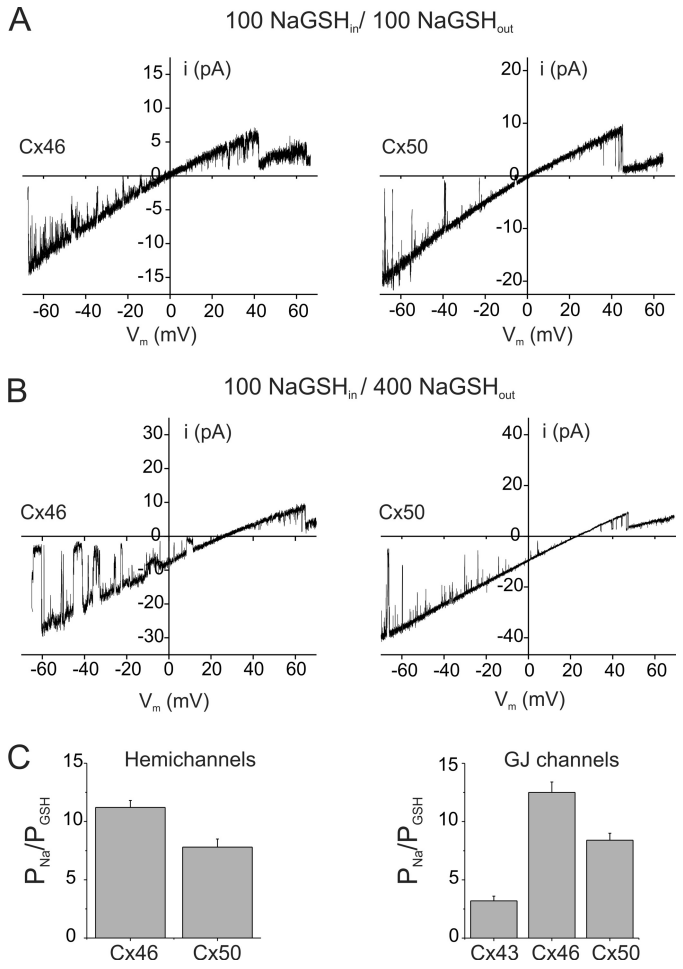

FIGURE 3. **GSH permeability of hemichannels and gap junction channels formed by Cx46 and Cx50.** *A* and *B,* single channel current-voltage relations for Cx46 (*left*) and Cx50 (*right*) hemichannels in symmetric NaGSH solutions (*A*) or 100:400 asymmetric NaGSH solutions (*B*) are shown. Cx46 and Cx50 hemichannel currents were recorded from excised inside-out patches in response to 8-s voltage ramps applied between −70 and +70 mV. In symmetric NaGSH solutions, Cx46 and Cx50 currents show inward rectification and reversed polarity at 0 mV. In asymmetric NaGSH solutions, reversal potentials for Cx46 and Cx50 hemichannel currents were below the equilibrium potential for Na^+ (~33 mV using activity coefficients), indicating that GSH permeates Cx46 and Cx50 channels. Inward rectification of the currents also increased in asymmetric solutions, consistent with the presence of higher Na^+ concentration on the extracellular side. *C,* permeability ratios (P_{Na}/P_{GSH}) of hemichannels (*left*) and gap junction channels (*right*) formed by connexins expressed in the lens. P_{Na}/P_{GSH} values for hemichannels and gap junction channels were calculated from reversal potentials in asymmetric 4:1 and 3:1 NaGSH gradients, respectively. Hemichannels and gap junction channels formed by Cx46 and Cx50 have a low but finite permeability to GSH relative to Na^+. In comparison, Cx43 forms channels that exhibit a higher permeability to GSH. Values represent the means ± S.E. from multiple recordings.

nels formed by Cx46 and Cx50. Anionic permeability of both unopposed hemichannels and gap junction channels formed by Cx46 and Cx50 was measured. The permeabilities of chloride and the larger GSH anion relative to Na^+ are shown in Figs. 2 and 3, respectively. Fig. 2 shows single hemichannel currents from Cx46- and Cx50-expressing oocytes in symmetric and asymmetric NaCl solutions in the bath and pipette. Single hemichannel current-voltage relations were obtained from excised patches in response to voltage ramps from −70 to +70 mV. In symmetric 100 mM NaCl solutions, Cx46 and Cx50 hemichannel currents reversed at 0 mV (Fig. 2*A*). Replacement of 100 mM NaCl in the solution bathing the extracellular face of hemichannels with 400 mM NaCl shifted reversal potentials toward the Na^+ equilibrium potential (Fig. 2*B*). In the illustrated recordings, reversal potentials in 4:1 gradients were found to be +20 mV for Cx46 and +16 mV for Cx50. Using reversal potentials from multiple patches and the Goldman-Hodgkin-Katz voltage equation, the P_{Na}/P_{Cl} values were calculated to be ~5 and ~3.3 for Cx46 and Cx50 hemichannels, respectively (Fig. 2*C*), indicating a preference of both connexin channel subtypes to cations. In addition, the presence of a higher concentration of salt on the extracellular side of the hemichannels changed the rectification of the *I-V* curves. In symmetrical salts, the Cx46 and Cx50 *I-V* relations display a

nearly 2:1 inward rectification over the ±70-mV range of the membrane potential, which has been attributed to the presence of fixed negative charges located toward the extracellular end of the hemichannel pore (32). In asymmetric NaCl gradients, the rectification was increased significantly due to the higher Na^+ concentration on the extracellular face of the hemichannel.

The charge selectivity of Cx46 and Cx50 cell-cell channels was similar to that of unopposed hemichannels, indicating that rearrangements that occur with docking do not influence the properties of the pore (Fig. 2*C*). Charge selectivity of Cx46 and Cx50 gap junction channels was determined from measurements of reversal potentials of junctional currents with patch pipettes that contained different salt solutions on each side of the junction (150 mM NaCl in one pipette and 50 mM NaCl in the second pipette). Selectivity of Cx43 gap junctions was also measured for comparison. E_{rev} values of Cx46 and Cx50 junctional currents were +17 and +12 mV, respectively, yielding P_{Na}/P_{Cl} values of 5:1 for Cx46 ($n = 3$) and 3:1 for Cx50 ($n = 4$) (Fig. 2*C*). The P_{Na}/P_{Cl} value for Cx46 gap junctions is in agreement with the P_K/P_{Cl} value of ~8 found by Trexler *et al.* (32), if one takes into account the lower aqueous mobility of Na^+ ions compared with K^+ ions. Cx43 gap junction channels showed no selectivity between Na^+ and Cl^- (E_{rev} ~0 mV), also consistent with previous studies which indicate that Cx43 forms nonselective gap junction channels (32).

The permeability of the larger GSH anion relative to Na^+ was similarly determined from reversal potential measurements. Recordings of Cx46 and Cx50 hemichannel currents in 1:1 and 4:1 NaGSH gradients are shown in Fig. 3, *A* and *B*, respectively. In the examples shown in Fig. 3, potentials at which Cx46 and Cx50 hemichannel currents reversed polarity were +26 and +24 mV, respectively. The P_{Na}/P_{GSH} values calculated from recordings of reversal potentials from multiple patches were ~11 for Cx46 ($n = 6$) and 8 ($n = 4$) for Cx50 hemichannels (Fig. 3*C*), indicating a lower permeability of the larger GSH anion compared with Cl^-. GSH permeability of Cx46 and Cx50 gap junctions was similarly low in magnitude, with P_{Na}/P_{GSH} values ranging from 8.4 for Cx50 to 12 for Cx46 (Fig. 3*B*). The mean E_{rev} values were 21.9 ± 1.5 for Cx46 ($n = 4$) and 20.1 ± 1.2 for Cx50 ($n = 5$), significantly different from the Na^+ equilibrium potential ($p < 0.05$). In comparison, Cx43 gap junctions, which are known to allow the passage of GSH (33), exhibited a relatively high permeability to the antioxidant molecule (P_{Na}/P_{GSH} of 3). These results indicate that both Cx46 and Cx50 are permeable to anionic GSH. Specifically, the finding that gap junctions formed by Cx46, which provides the majority of the coupling in mature fiber cells, are permeable to GSH indicates that diffusion of the anti-oxidant could occur from the lens outer cortex (region of high concentration) to the nucleus.

We also determined whether Cx46 and Cx50 gap junctions allow the passage of oxidized glutathione, GSSG, a divalent anion at pH 7.4. Fig. 4 shows junctional currents obtained from cell pairs expressing Cx46 and Cx50 in a 3:1 gradient of Na_2GSSG. Voltage pulses were applied to the cell containing the higher salt concentration. Single channel current rectified with the larger current when the cell containing the higher salt concentration was made positive. Measured reversal potentials for Cx46 and Cx50 junctions were close to the Na^+ equilibrium

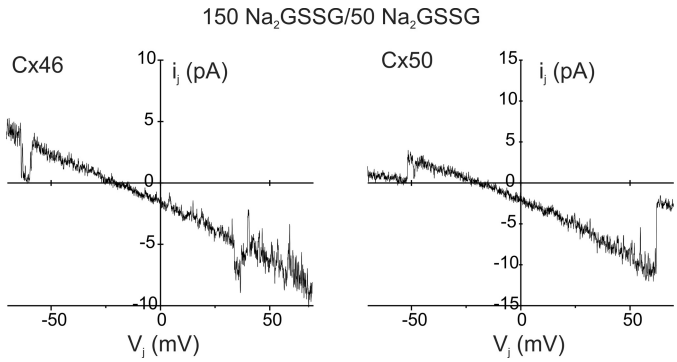

FIGURE 4. **Permeation of GSSG in Cx46 and Cx50 gap junction channels is extremely low.** Recordings of Cx46 (*left*) and Cx50 (*right*) junctional currents from cell pairs in which one patch pipette contained 150 mM Na_2GSSG and the other 50 mM Na_2GSSG. Junctional currents were elicited by the application of voltage ramps to the cell containing 150 mM Na_2GSSG. Junctional current was rectified with more current at positive voltage pulses. Reversal potentials of the Cx46 and Cx50 junctional currents were close to the equilibrium potential for Na^+ suggesting extremely low GSSG permeability. Similar results were obtained from three cell pairs.

potential (~28 mV) under these conditions, suggesting a very low permeability to GSSG. The mean E_{rev} values were 26.4 ± 2.5 for Cx46 ($n = 3$) and 27.2 ± 1.9 for Cx50 ($n = 3$). Permeation of GSSG in Cx46 and Cx50 hemichannels, measured using larger 4:1 gradients, was also extremely low (data not shown).

GSH Levels in the Lens Nucleus Are Markedly Reduced in the Absence of Cx46—The electrophysiological measurements indicated that Cx46 gap junctions permit the passage of GSH. Thus, it is likely that GSH levels in the lens core are dependent on the presence of Cx46. To determine the importance of the *in vitro* measurements of GSH permeability *in vivo*, we measured the levels of the anti-oxidant in lenses obtained from connexin knock-out (KO) mice. We initially measured GSH levels in Cx46 KO and Cx50 KO lenses obtained from mice at 6 months of age. GSH levels in whole lens homogenates obtained from Cx50 KO were similar to those found in wild type (data not shown). In contrast, the absence of Cx46 caused a significant reduction in GSH content by ~45% (data not shown). Because Cx46 provides the majority of the coupling of inner fiber cells, we determined whether this reduction of GSH in Cx46 KO occurred specifically in the nucleus. Lenses were separated into two fractions, with one fraction containing the nucleus and the other consisting of the outer cortex and epithelium. The amount of GSH normalized to wet weight in the two fractions was measured and is shown in Fig. 5. In WT lenses, the GSH content was high in the cortical fraction, but much lower in the nucleus, confirming the existence of a regional difference in GSH levels (Fig. 5). The absence of Cx46 or Cx50 did not significantly affect GSH levels in the cortex (Fig. 5*A*). In contrast, as shown in Fig. 5*B*, GSH levels were significantly reduced in the nuclear fraction of lenses obtained from Cx46 KO mice ($p < 0.05$). The reduction amounted to ~96% on average (0.95 ± 0.1 μmol/g wet weight in WT lenses ($n = 5$) to 0.03 ± 0.01 μmol/g wet weight in Cx46 KO ($n = 5$)). Knock-out of Cx50 did not significantly affect GSH levels in the nucleus ($p > 0.05$). Our studies used mice in the C57 black background in which genetic ablation of Cx46 causes a mild cataract even at 6 months of age. Thus, these biochemical experiments are unlikely to be affected by the presence of cataracts. Nevertheless, we measured GSH

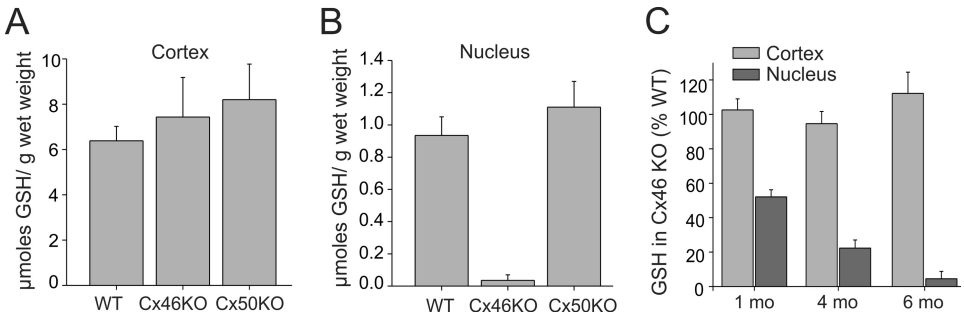

FIGURE 5. **Cx46 is essential for the maintenance of adequate levels of GSH in the lens nucleus.** *A* and *B,* amount of GSH normalized to wet weight in the cortical (*A*) and nuclear (*B*) fraction of lenses obtained from wild type (*WT*), Cx46 knock-out (*Cx46KO*), and Cx50 knock-out (*Cx50KO*) are shown. In WT lenses, GSH levels were high in the cortical fraction but much lower in the nucleus. The absence of Cx46 or Cx50 did not significantly affect GSH levels in the cortex. In comparison, knock-out of Cx46 but not Cx50 caused a robust reduction in GSH levels in the nuclear fraction. Values represent means ± S.E. from five lenses each obtained from wild type, Cx46 KO, and Cx50 KO mice. *C,* decrease in GSH in C, 4, and 6 months (*mo*) of age. Substantial reductions in GSH levels were found in the nuclear fraction but not the cortical fraction of Cx46 KO lenses at all developmental time points. *N* values are given in the text.

levels in Cx46 KO mice at 1 and 4 months of age. As shown in Fig. 5*C*, substantial reductions in GSH levels were found at these earlier time points (Fig. 5*C*). In 1-month-old lenses, GSH levels decreased by 52 ± 4% ($n = 4$). By 4 months of age, the decrease amounted to 78 ± 5% ($n = 6$). These results provide a unique role for Cx46 gap junctions in the maintenance of adequate GSH levels in the nucleus.

Contribution of the Extracellular Pathway for Maintenance of GSH Levels in the Nucleus—We measured the contribution of the lens circulation to intracellular GSH levels by inhibiting Na^+-K^+-ATPase, which ultimately drives the circulating current. Previous studies showed that inhibition of the Na^+-K^+-ATPase by ouabain or by replacement of extracellular Na^+ with K^+ significantly reduced the lens hydrostatic pressure and disrupted the lens circulation (16). WT whole lenses were incubated for 3 h in artificial aqueous humor (AAH control) and in AAH containing 1 mM ouabain or in sodium-free AAH, and GSH content was measured in cortical and nuclear fractions of lenses. As shown in Fig. 6*A*, cortical GSH levels remained unaffected by the inhibition of the Na^+-K^+ ATPase. In the nuclear fraction of lenses incubated with ouabain, the GSH content was ~35% higher than the values found in control lenses (0.40 ± 0.005 μmol/g wet weight; $n = 4$ in ouabain *versus* 0.29 ± 0.003 μmol/g wet weight; $n = 4$ in control; $p < 0.05$). Similar changes were observed in lenses ($n = 4$) incubated in Na^+-free conditions (Fig. 6*B*). These results indicate that the contribution of the extracellular pathway to GSH delivery to the nucleus is minimal.

Modeling the GSH Concentration in the Lens—We modeled the radial distribution of GSH in the lens taking into account that GSH diffusion is influenced by the concentration gradient, the voltage gradient (conduction), and the hydrostatic pressure gradient (advection). Any intracellular membrane-impermeant solute that is synthesized at some specific location within the lens (like GSH synthesis in surface cells) will diffuse away from the site of synthesis at a rate that depends on the rate of synthesis. If the rate of synthesis is relatively slow, then conduction and advection may significantly alter the diffusion gradient. However, for GSH the rate of synthesis in surface cells is relatively high, and the diffusion gradient is not appreciably affected by either conduction or advection. The consumption rates of GSH in the different regions of the lens are unknown.

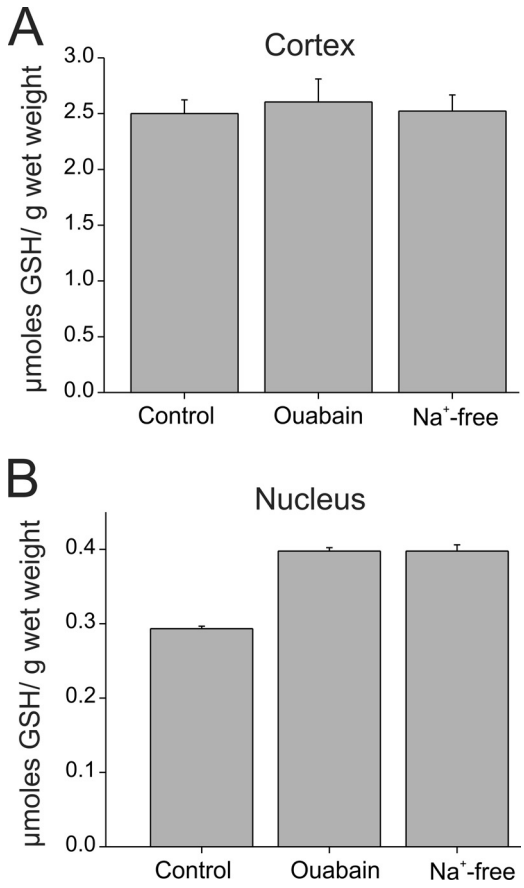

FIGURE 6. **Contribution of the lens circulation to the delivery of GSH to the nucleus is minor.** *A* and *B,* amount of GSH normalized to wet weight in the cortical (*A*) and nuclear (*B*) fraction of wild type lenses incubated with inhibitors of the Na^+-K^+-ATPase that drives the lens circulation. Na^+-K^+-ATPase was inhibited either with ouabain (1 mM) or by completely replacing Na^+ in the external AAH solution with K^+. Disruption of the lens circulation did not reduce GSH levels in the cortical or the nuclear fraction. Ouabain and Na^+-free AAH caused a slight increase in GSH levels in the nucleus. Values represent means ± S.E. from four lenses in each condition.

Therefore, we initially modeled the diffusion of GSH assuming that consumption rates are uniform throughout the lens. Fig. 7*A* shows the GSH concentration profile from the periphery to the center using the uniform consumption model calculation (supplemental Equations 21–25). Calculation of the GSH concentration gradient due to diffusion only (the G^0 solution in

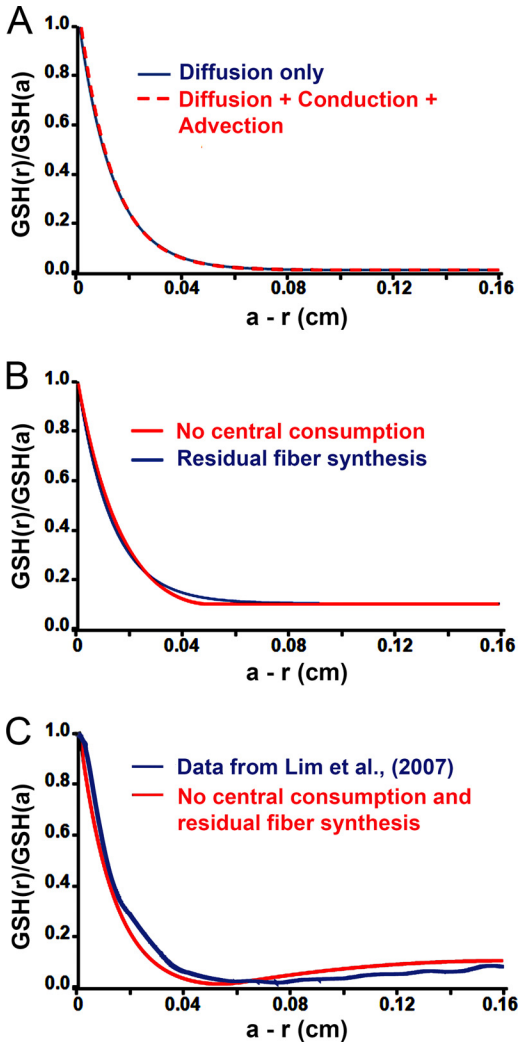

FIGURE 7. **Different models of GSH diffusion compared with experimental data (Lim *et al.* (5)).** *A,* overplot of model calculations based on the full model in red ($G^{(0)} + \epsilon G^{(1)}$) given in supplemental Equations 17 and 21, overplotted with a model of diffusion only in *blue* ($G^{(0)}$) given in supplemental Equation 17. The two models differ by less than a line width in this diffusion dominated system, so the correction $\epsilon G^{(1)}$ is ignored in the other panels. *B,* an overplot of two new models for diffusion of GSH that does not go to zero in central fiber cells. In one model (*red*), there is assumed to be no consumption of GSH in fiber cells farther into the lens than $a - r = 0.05$ cm. In the other model (*blue*), there is assumed to be residual *de novo* synthesis of GSH in all fiber cells. *C,* third new model for diffusion of GSH. In this model (*red*), there is assumed to be no consumption of GSH in fiber cells farther into the lens than $a - r = 0.05$ cm, and there is assumed to be residual *de novo* synthesis of GSH in all fiber cells. The plot from model calculations overlaps closely with experimental data obtained by Lim *et al.* (5) on the diffusion gradient for GSH in a rat lens (*blue*). The data plot shown in *blue* was adapted from Fig. 3*A* of Lim *et al.* (5).

supplemental material) is plotted with the equation that includes both conduction and advection (the $G^{(0)} + \epsilon G^{(1)}$ solution in the supplemental material). The two curves essentially superimpose, indicating that conduction and advection are negligible in this diffusion dominated system.

The steep decline in GSH concentration in the outer cortex implies a high rate of consumption; however, a large consumption in central fiber cells will cause the GSH concentration to decline to zero about 500 μm from the surface. This is inconsistent with previous studies that show that GSH levels in the core are low, but non-zero (1, 2, 5, 7). For example, mapping of GSH levels using anti-GSH antibodies indicated that the levels of GSH and its precursor amino acids were high in the outer cortex and declined to a non-zero level ~500 μm from the periphery (5). In the core, the mapping studies actually showed a slight increase in GSH levels compared with the levels in the inner cortex (see plot in blue in Fig. 7*C*, which shows data adapted from Fig. 3*A* of Lim *et al.* (5)). One possible reason for the difference between the model and the studies by Lim *et al.* (5) is that the rate of consumption is not uniform, but instead it declines to a lower rate in central fibers. Under these conditions, the GSH concentration would be expected to be non-zero. Another possibility is that there is small residual *de novo* synthesis or uptake of GSH in all fiber cells. To distinguish between these possibilities, we constructed two additional models, one in which the central consumption was assumed to be zero and the other in which *de novo* synthesis or uptake occurs in central fiber cells at a low rate (see supplemental material). These models approximated the radial GSH profile (Fig. 7*B*) but did not fit the slight increase in GSH seen by Lim *et al.* (5) in the nucleus (see Fig. 7*C*).

To fit the data of Lim *et al.* (5), we ultimately had to combine both models, *i.e.* a major reduction in GSH consumption in the central fibers along with some residual synthesis or uptake of GSH in all fiber cells (Fig. 7*C*, *plot in red*). GSH that is synthesized in the central cells is not consumed, so it diffuses back toward more peripheral fiber cells where a higher rate of consumption is occurring. This creates the negative slope in GSH concentration between $r = 0$ and $r = 0.11$ cm.

DISCUSSION

In this study, we showed that Cx46 and Cx50 channels are permeable to GSH. Thus, GSH is expected to passively diffuse from the outer cortex, where a high concentration is established by the synthesis (3, 4) and/or uptake by specific transporters (34, 35), to the nucleus. The difference in the membrane potentials of the outer and inner fiber cells also favors diffusion. Intracellular water flow from the lens center to surface opposes diffusion, but as shown in our model calculations below, the contribution of the voltage or advection is small in the presence of a large concentration gradient. Consistent with diffusion occurring via a gap junctional pathway, we found that deletion of Cx46, the connexin isoform that provides bulk of the coupling between fiber cells in the core, led to a marked and selective decrease in GSH levels in the lens core. This reduction was not due to a disruption of the lens circulation, because blocking the lens circulation independently by inhibiting the Na^+-K^+-ATPase had an opposite effect on GSH levels in the nucleus. These results indicate that delivery of GSH to the nucleus is dependent on the presence of Cx46 gap junctions.

Permeation of GSH and GSSG—GSH is a low molecular metabolite with dimensions ~14 × 3 × 5 Å, within the size exclusion limit of the connexin channel pore (36). Direct assessments of charge selectivity indicated that the channels formed by the three connexin isoforms expressed in the lens display distinct differences in permeability to GSH and to the smaller Cl^-. Intercellular channels formed by Cx43 showed little charge selectivity and were highly permeable to GSH, consistent with previous studies that indicate Cx43 channels are per-

meable to a variety of endogenous metabolites, including ATP, and to a range of large anionic tracer molecules containing one or more negative charges (*e.g.* Lucifer yellow and calcein) (37, 38). In contrast, gap junctions and hemichannels formed by lens fiber cell connexins were 3–5-fold selective for Na^+ over Cl^-. The charge selectivity in Cx46 has been ascribed to the presence of fixed negative charges in the first extracellular loop (32), causing cations to partition into the channel and anions to partition out. A negative charge on the interior channel wall is also likely to be responsible for the higher cation selectivity of Cx50. The degree of rectification of single Cx46 and Cx50 hemichannel currents is similar (27, 32). In addition, Cx50 shares a significant sequence homology to Cx46 in the extracellular loops. The larger GSH anion was 8–12-fold less permeant than Na^+. The lower selectivity of GSH anion compared with Cl^- presumably reflects the influence of both surface charge effects and size exclusion effects.

GSH participates in multiple enzymatic reactions in the lens. GSSG formed in these reactions is regenerated to GSH by the enzymatic action of glutathione reductase, whose activity is high in the outer cortex (3, 4). But the activity of glutathione reductase is much lower in central fiber cells (3, 4). Thus, GSSG formed in inner fiber cells is believed to diffuse back to the periphery where it can be reduced to regenerate GSH. However, GSSG permeation through fiber cell gap junction channels was not detectable in our studies. Although it is possible that gap junctions may allow diffusion of the divalent ion to the periphery from the center because the coupling conductance of fiber cells is typically very high, other pathways for GSSG efflux/breakdown might operate in the lens. Cell-cell diffusion of molecules in the lens may also be mediated by membrane fusions between adjacent fiber cells (39, 40). Unlike gap junction channels, which exclude molecules above 1 kDa, membrane fusions can allow the diffusion of very large molecules such as green fluorescent protein (GFP) and Alexa 488 conjugated to dextran between adjacent cells (39, 40). These fusions have been identified in adult lenses from several species, including humans and rodents, and require the presence of Lim2 (also known as MP20) (41). However, these fusions appear to occur between fibers in concentric spherical shells and do not provide a continuous path from the lens center to the surface (37). Whether GSSG efflux to surface cells occurs through cell-cell fusions, gap junctions or an alternative mechanism requires additional studies.

Cx46 and the Age-dependent Decrease in GSH Levels in the Lens Nucleus—The decrease in GSH levels in the aging lens has been attributed to a number of factors, including reduced activity of enzymes involved in GSH synthesis (4). However, this reduction does not appear to be sufficient to account for the marked age-dependent decline in GSH levels in the lens core (19). For example, in advanced stages of cataract when GSH levels in the nucleus decline significantly, the anti-oxidant levels remain sufficiently high in the outer cortex (42). A barrier to the diffusion of GSH was shown to develop with age (19). Although the molecular substrate of the barrier was not explicitly defined, alterations in the conductance and permeability properties of Cx46 gap junctions may explain why GSH diffusion is slowed with aging. In the young lens, the low GSH permeability through Cx46 channels is offset by the high levels of coupling conductance (average of 0.5 siemens/cm^2) (14) in the lens core, allowing adequate levels of the anti-oxidant to be delivered to the central fiber cells. But with aging, coupling conductance decreases by ~70% in the inner cortex and nucleus (43). This reduction in coupling, in combination with the diminished efficiency of GSH synthesis in the outer cortex, is expected to significantly limit GSH diffusion from the outer cortex to the central cells. What causes the reduction in coupling is not known, but recent studies show that Cx46 undergoes a number of post-translational modifications, including truncations in the N terminus and cytoplasmic loop of the protein, which are likely to cause channels to be nonfunctional (44).

Summary of Modeling Results—Modeling of biological data can never be exact, so one tries to identify the essential physical processes that are affecting the data. There is clearly diffusion of intracellular GSH toward the center of the lens from its site of synthesis in surface cells, and GSH is clearly being consumed as it diffuses into the lens. These conclusions can explain the data from fiber cells in the outer cortex; however, they are not sufficient to describe the data from central fiber cells. To fit those data, we ultimately had to postulate a major reduction in GSH consumption in central fibers along with some residual synthesis or uptake of GSH in all fiber cells. Lim *et al.* (5) were unable to detect membrane transporters for GSH in fiber cells; however, they did report uptake of some precursors to synthesis. Therefore, *de novo* synthesis appears to be the most likely cause of the small negative slope in the central concentration of GSH. The rate of synthesis used for the graph in Fig. 7*C* was 29 nM/s, so it is indeed quite small yet capable of generating about a 2 mM gradient from the center ($r = 0$) to fiber cells at $r = 0.11$ cm; this gradient is generated in the absence of consumption. In contrast, the rate of synthesis in the lens epithelium can be estimated from the slope of the peripheral concentration gradient; it is about 92 μM/s or some 3000 times greater than synthesis in central cells. These are the essential physical processes that have been identified through modeling as necessary to explain the data of Lim *et al.* (5) in Fig. 7*C*.

In summary, our results demonstrate an important role for gap junction channels in the delivery of glutathione in the lens. The decline in GSH levels in the lens nucleus that occurs with aging is considered to be a key initiating factor in the formation of senile cataracts. The involvement of gap junctions in this age-dependent reduction of GSH may lead to identification of new therapeutic strategies (*e.g.* modulation of intercellular communication) for delaying the progression of age-related nuclear cataracts.

Acknowledgment—We thank Dr. Vytas Verselis for helpful discussions during the course of this study.

REFERENCES

1. Giblin, F. J. (2000) Glutathione: a vital lens antioxidant. *J. Ocul. Pharmacol. Ther.* **16,** 121–135
2. Reddy, V. N. (1990) Glutathione and its function in the lens–an overview. *Exp. Eye Res.* **50,** 771–778
3. Ganea, E., and Harding, J. J. (2006) Glutathione-related enzymes and the eye. *Curr. Eye Res.* **31,** 1–11

4. Rathbun, W. B. (1984) Lenticular glutathione synthesis: rate-limiting factors in its regulation and decline. *Curr. Eye Res.* **3,** 101–108
5. Lim, J., Li, L., Jacobs, M. D., Kistler, J., and Donaldson, P. J. (2007) Mapping of glutathione and its precursor amino acids reveals a role for GLYT2 in glycine uptake in the lens core. *Invest. Ophthalmol. Vis. Sci.* **48,** 5142–5151
6. Lou, M. F. (2003) Redox regulation in the lens. *Prog. Retin. Eye Res.* **22,** 657–682
7. Truscott, R. J. (2000) Age-related nuclear cataract: a lens transport problem. *Ophthalmic Res.* **32,** 185–194
8. Bova, L. M., Sweeney, M. H., Jamie, J. F., and Truscott, R. J. (2001) Major changes in human ocular UV protection with age. *Invest. Ophthalmol. Vis. Sci.* **42,** 200–205
9. Dickerson, J. E., Jr., and Lou, M. F. (1993) A new mixed disulfide species in human cataractous and aged lenses. *Biochim. Biophys. Acta* **1157,** 141–146
10. Harding, J. J. (1969) Glutathione-protein mixed disulphides in human lens. *Biochem. J.* **114,** 88P–89P
11. Lou, M. F., and Dickerson, J. E., Jr. (1992) Protein-thiol mixed disulfides in human lens. *Exp. Eye Res.* **55,** 889–896
12. Candia, O. A., Mathias, R., and Gerometta, R. (2012) Fluid circulation determined in the isolated bovine lens. *Invest. Ophthalmol. Vis. Sci.* **53,** 7087–7096
13. Mathias, R. T., Kistler, J., and Donaldson, P. (2007) The lens circulation. *J. Membr. Biol.* **216,** 1–16
14. Mathias, R. T., Rae, J. L., and Baldo, G. J. (1997) Physiological properties of the normal lens. *Physiol. Rev.* **77,** 21–50
15. Baldo, G. J., and Mathias, R. T. (1992) Spatial variations in membrane properties in the intact rat lens. *Biophys. J.* **63,** 518–529
16. Gao, J., Sun, X., Moore, L. C., White, T. W., Brink, P. R., and Mathias, R. T. (2011) Lens intracellular hydrostatic pressure is generated by the circulation of sodium and modulated by gap junction coupling. *J. Gen. Physiol.* **137,** 507–520
17. Donaldson, P. J., Musil, L. S., and Mathias, R. T. (2010) Point: A critical appraisal of the lens circulation model–an experimental paradigm for understanding the maintenance of lens transparency? *Invest. Ophthalmol. Vis. Sci.* **51,** 2303–2306
18. Sweeney, M. H., Garland, D. L., and Truscott, R. J. (2003) Movement of cysteine in intact monkey lenses: the major site of entry is the germinative region. *Exp. Eye Res.* **77,** 245–251
19. Sweeney, M. H., and Truscott, R. J. (1998) An impediment to glutathione diffusion in older normal human lenses: a possible precondition for nuclear cataract. *Exp. Eye Res.* **67,** 587–595
20. Gong, X., Baldo, G. J., Kumar, N. M., Gilula, N. B., and Mathias, R. T. (1998) Gap junctional coupling in lenses lacking α3 connexin. *Proc. Natl. Acad. Sci. U.S.A.* **95,** 15303–15308
21. Paul, D. L., Ebihara, L., Takemoto, L. J., Swenson, K. I., and Goodenough, D. A. (1991) Connexin46, a novel lens gap junction protein, induces voltage-gated currents in nonjunctional plasma membrane of *Xenopus* oocytes. *J. Cell Biol.* **115,** 1077–1089
22. White, T. W., Bruzzone, R., Goodenough, D. A., and Paul, D. L. (1992) Mouse Cx50, a functional member of the connexin family of gap junction proteins, is the lens fiber protein MP70. *Mol. Biol. Cell* **3,** 711–720
23. White, T. W., Goodenough, D. A., and Paul, D. L. (1998) Targeted ablation of connexin50 in mice results in microphthalmia and zonular pulverulent cataracts. *J. Cell Biol.* **143,** 815–825
24. Baldo, G. J., Gong, X., Martinez-Wittinghan, F. J., Kumar, N. M., Gilula, N. B., and Mathias, R. T. (2001) Gap junctional coupling in lenses from α(8) connexin knockout mice. *J. Gen. Physiol.* **118,** 447–456
25. Martinez-Wittinghan, F. J., Sellitto, C., Li, L., Gong, X., Brink, P. R., Mathias, R. T., and White, T. W. (2003) Dominant cataracts result from incongruous mixing of wild-type lens connexins. *J. Cell Biol.* **161,** 969–978
26. Martinez-Wittinghan, F. J., Sellitto, C., White, T. W., Mathias, R. T., Paul, D., and Goodenough, D. A. (2004) Lens gap junctional coupling is modulated by connexin identity and the locus of gene expression. *Invest. Ophthalmol. Vis. Sci.* **45,** 3629–3637
27. Srinivas, M., Kronengold, J., Bukauskas, F. F., Bargiello, T. A., and Verselis, V. K. (2005) Correlative studies of gating in Cx46 and Cx50 hemichannels and gap junction channels. *Biophys. J.* **88,** 1725–1739
28. Gong, X., Li, E., Klier, G., Huang, Q., Wu, Y., Lei, H., Kumar, N. M., Horwitz, J., and Gilula, N. B. (1997) Disruption of α3 connexin gene leads to proteolysis and cataractogenesis in mice. *Cell* **91,** 833–843
29. Gong, X., Agopian, K., Kumar, N. M., and Gilula, N. B. (1999) Genetic factors influence cataract formation in α3 connexin knockout mice. *Dev. Genet.* **24,** 27–32
30. Srinivas, M., Costa, M., Gao, Y., Fort, A., Fishman, G. I., and Spray, D. C. (1999) Voltage dependence of macroscopic and unitary currents of gap junction channels formed by mouse connexin50 expressed in rat neuroblastoma cells. *J. Physiol.* **517,** 673–689
31. Wang, H. Z., and Veenstra, R. D. (1997) Monovalent ion selectivity sequences of the rat connexin43 gap junction channel. *J. Gen. Physiol.* **109,** 491–507
32. Trexler, E. B., Bukauskas, F. F., Kronengold, J., Bargiello, T. A., and Verselis, V. K. (2000) The first extracellular loop domain is a major determinant of charge selectivity in connexin46 channels. *Biophys. J.* **79,** 3036–3051
33. Goldberg, G. S., Lampe, P. D., and Nicholson, B. J. (1999) Selective transfer of endogenous metabolites through gap junctions composed of different connexins. *Nat. Cell Biol.* **1,** 457–459
34. Kannan, R., Yi, J. R., Tang, D., Zlokovic, B. V., and Kaplowitz, N. (1996) Identification of a novel, sodium-dependent, reduced glutathione transporter in the rat lens epithelium. *Invest. Ophthalmol. Vis. Sci.* **37,** 2269–2275
35. Kannan, R., Yi, J. R., Zlokovic, B. V., and Kaplowitz, N. (1995) Molecular characterization of a reduced glutathione transporter in the lens. *Invest. Ophthalmol. Vis. Sci.* **36,** 1785–1792
36. Maeda, S., Nakagawa, S., Suga, M., Yamashita, E., Oshima, A., Fujiyoshi, Y., and Tsukihara, T. (2009) Structure of the connexin 26 gap junction channel at 3.5 Å resolution. *Nature* **458,** 597–602
37. Harris, A. L. (2001) Emerging issues of connexin channels: biophysics fills the gap. *Q. Rev. Biophys.* **34,** 325–472
38. Harris, A. L. (2007) Connexin channel permeability to cytoplasmic molecules. *Prog. Biophys. Mol. Biol.* **94,** 120–143
39. Shestopalov, V. I., and Bassnett, S. (2003) Development of a macromolecular diffusion pathway in the lens. *J. Cell Sci.* **116,** 4191–4199
40. Shi, Y., Barton, K., De Maria, A., Petrash, J. M., Shiels, A., and Bassnett, S. (2009) The stratified syncytium of the vertebrate lens. *J. Cell Sci.* **122,** 1607–1615
41. Shi, Y., De Maria, A. B., Wang, H., Mathias, R. T., FitzGerald, P. G., and Bassnett, S. (2011) Further analysis of the lens phenotype in Lim2-deficient mice. *Invest. Ophthalmol. Vis. Sci.* **52,** 7332–7339
42. Truscott, R. J., and Augusteyn, R. C. (1977) The state of sulfhydryl groups in normal and cataractous human lenses. *Exp. Eye Res.* **25,** 139–148
43. Gao, J., Wang, H., Sun, X., Varadaraj, K., Li, L., White, T. W., and Mathias, R. T. (2013) The effects of age on lens transport. *Invest. Ophthalmol. Vis. Sci.* **54,** 7174–7187
44. Wang, Z., and Schey, K. L. (2009) Phosphorylation and truncation sites of bovine lens connexin 46 and connexin 50. *Exp. Eye Res.* **89,** 898–904